Carbohydrate Polymers 117 (2015) 392–399

Contents lists available at ScienceDirect

Carbohydrate Polymers

journal homepage: www.elsevier.com/locate/carbpol

Characterization of new natural cellulosic fiber from *Cissus quadrangularis* stem

S. Indran, R. Edwin Raj*

Department of Mechanical Engineering, St. Xavier's Catholic College of Engineering, Chunkankadai, Nagercoil 629003, Tamil Nadu, India

ARTICLE INFO

Article history:
Received 9 May 2014
Received in revised form
19 September 2014
Accepted 23 September 2014
Available online 7 October 2014

Keywords:
Cissus quadrangularis
Fibers
Chemical properties
Mechanical properties
Thermal properties
SEM

ABSTRACT

Polymer composite has contributed tremendously for energy efficient technologies in automotive and aero industries. Environmental and health concerns related to the carcinogenic nature of artificial fiber in polymer composite needs a retrofit. Eco friendly natural cellulosic fiber extract from the stem of *Cissus quadrangularis* plant is extensively characterized to consider as a viable alternative for man-made hazardous fibers. Anatomical study, chemical analysis, physical analysis, FTIR, XRD, SEM analysis and thermo gravimetric analysis were done to establish the certainty of using them as reinforcement fiber. Its light weight and the presence of high cellulose content (82.73%) with very little wax (0.18%) provide high specific strength and good bonding properties in composite manufacturing. The flaky honeycomb outer surface revealed through electron microscopy contributes for high modulus in CQ stem fiber and thermo gravimetric analysis ensures thermal stability up to 270 °C, which is within the polymerization process temperature.

1. Introduction

The applicability and adaptability of fiber reinforced polymer composite materials (FRP) for various industrial applications, especially in automotive and aerospace industries are highly appreciated and supported by researchers. Synthetic fibers such as glass fiber, aramid, ceramic fiber, carbon fiber, etc., are not only costly, but also carcinogenic in prolonged exposure. Studies have shown occurrence of DNA damage at high dosage and the tendency for genotoxic and cytotoxic effect in persons exposed to glass fiber particles. Furthermore, reduction in microvilli membrane and oxidative stress on mesothelial cells were also reported (Cavallo et al., 2004). Stimulation of T-cell was observed while working with rock wool. Similarly both T-cell and B-cell stimulation were observed in fiber glass workers causing depression of lymphocyte in blood. Noted increase in expression of eosinophil activators leading to allergy was also observed in fiber glass workers. Exposure to mineral fibers relevantly increases the expression and function of adhesion molecules, which was pathologically verified (Tulinska et al., 2004).

Synthetic fibers are in general non-degradable, whereas natural fibers are degradable and non-pollutant to the environment. Since the global warming potential and toxicity of the environment are increasing it is good to look up to the nature and to learn what it can offer for our sustainable living conditions. Most of the properties of natural fibers are excellent, whereas some are negotiable, which makes them attractive to replace synthetic fibers in all applications (Thiruchitrambalam, Athijayamani, Sathiyamurthy, & Thaheer, 2010). Some of the natural fibers investigated in literature have reported low specific strength in comparison with synthetic fibers due to its texture and hydrophilic nature (Reddy, Uma, Mukul, Song, & Varada Rajulu, 2013; Mehta, Mohanty, Misra, & Drzal, 2004). Many natural fibers such as coir, bamboo, jute, borassus, flax, banana, etc., were characterized for their mechanical properties (Faruk, Bledzkia, Finkb, & Sain, 2012; Sathishkumar, Navaneetha krishnan, & Shankar, 2012). Jayant and Palit (2013) reported that "It is hard to define the quality of a bast fiber". The *Cissus quadrangularis* stem fiber (CQSF) is characterized for the first time comprehensively in this paper. Its mechanical properties are on par with synthetic fibers and some of them are even better when their densities are considered.

C. quadrangularis (CQ) is a perennial plant belonging to the *Vitaceae* (grape) family. It is commonly known as Perandai in tamil language, which has its origin in India/Srilanka, however it is widely available in Africa, Arabia and south–east Asia. CQ is a climber reaching to a height of 2.5 m and has quadrangular sectioned branches with internodes of 1.5–1.8 cm width and 10–15 cm long (Indran, Edwin Raj, & Sreenivasan, 2014). They grow rapidly even in

* Corresponding author Tel.: +91 9442054535; Fax: +91 04652 233982.
E-mail address: redwinraj@gmail.com (R.E. Raj).

http://dx.doi.org/10.1016/j.carbpol.2014.09.072
0144-8617/

Fig. 1. *Cissus quadrangularis* plant with its extracted stem fiber.

very adverse weather conditions. CQ is long known for its medicinal values and is widely used to strengthen bones and to treat ligament tears. CQSF is extensively investigated for its anatomy, mechanical, thermal, chemical and physical properties. The experimental results were significant and encouraging for employing CQSF as a reinforcing material in the manufacture of polymer composite.

2. Materials and methods

2.1. Extraction of CQ stem fiber

The CQ plants were collected from Asarivilai, Kanyakumari District, Tamil Nadu, India. They were soaked in water for two weeks to undergo microbial degradation. They were then washed and dried in natural sunlight to remove moisture content. Once the fleshy layer gets withered, combing was done with a metal brush to remove unwanted particles from the fiber surface and long uniform fibers were obtained (Fig. 1).

2.2. CQ stem anatomy

Isolated healthy stems were examined under the polarized microscope to study its microstructure. The stems were cut into small pieces (10 × 10 mm) and immersed in FAA solution (5 ml formaldehyde + 5 ml acetic acid + 90 ml 70% ethyl alcohol) for 24 h to preserve the tissues. They were then dehydrated through a graded tertiary butyl alcohol series and embedded in paraffin (Sass, 1940). Microstructural specimens were then prepared by sectioning them of 10–12 μm size using rotary microtome. It was then affixed to a glass slide stained with a mixture of toluidine blue solution for clarity picture (O'Brien, Feder, & McCull, 1964). Polarized light microscope unit (Nikon, Japan) was used for polarized light microscope histochemistry study.

2.3. Chemical properties

The cellulose, hemicellulose and lignin contents of CQSFs were determined using standard test procedures (Doree, 1950; Pearl, 1967). The sample was dried in an oven at 104 °C for 4 h to determine the moisture content (Sreenivasan, Somasundaram, Ravindran, Manikandan, & Narayanasamy, 2011). The wax content was quantified as per the standard protocol (Conrad, 1944). Samples examined on wet and dry basis, especially on soxhlet apparatus were 2–5% and 6–8% error, respectively, are bound to occur, which are acceptable (Satyanarayana, Thais,, Lucas, & Juliana, 2013).The chemical compositions of other natural cellulosic fibers are compared from the available data and tabulated in Table 1 (Ku, Wang, Pattarachaiyakoop, & Trada, 2011; Faruk et al., 2012; Jawaid & Abdul Khalil, 2011; Sathishkumar et al., 2012; Hejazi, Sheikhzadeh, Abtahi, & Zadhoush, 2012; Fernando Pacheco-Torgal & Jalali, 2011; Ho et al., 2012; Dittenber & Ganga Rao, 2012; Mantia & Morreale, 2011; Koronis, Silva, & Fontul, 2013; Sreenivasan et al., 2011; Satyanarayana, Sukumaran, Mukherjee, Pavithran, & Pillai, 1990; Saravanakumar, Kumaravel, Nagarajan, Sudhakar, & Baskaran, 2013; Sathishkumar, Navaneethakrishnan, Sankar, Rajasekar, & Rajini, 2013; Indran et al., 2014).

2.4. Physical properties

2.4.1. Fiber density

The density was determined by liquid immersion test using pycnometer with tolune (Béakou, Ntenga, Lepetit, Ateíba, & Ayina, 2008). The fibers were dry stored for further testing in a desiccator containing silica. The density of CQSF was calculated using the relation:

$$\rho_{CQSF} = \frac{(m_2 - m_1)}{(m_3 - m_1)(m_4 - m_2)}\rho_t \quad (1)$$

where, ρ_{CQSF} is the density of CQSF (g/cm^3), ρ_t is the density of toluene (g/cm^3), m_1 is the mass of empty pycnometer (kg), m_2 is the mass of pycnometer with fibers (kg), m_3 is the mass of pycnometer with toluene (kg) and m_4 is the mass of pycnometer with fibers and toluene (kg).

2.4.2. Single CQSF tensile test

The tensile tests for CQSF were conducted using INSTRON 5500R type UTM as per the ASTM D 3822-07 standard. Tests were conducted at various gauge lengths of 10 mm, 20 mm, 30 mm, 40 mm and 50 mm with 20 samples for each gauge length. A constant cross head speed of 0.1 mm/min was used for the testing and it was conducted at an ambient temperature of ~28 °C and relative humidity of ~65%.

2.5. Fourier transform infrared spectroscopy (FTIR)

Perkin Elmer Spectrum RXI Fourier transform infrared spectrometer was used to derive the FTIR spectra of the CQSFs in KBr matrix with a scan rate of 32 scans per minute at a resolution of 2 cm^{-1} in the wave number region between 400 cm^{-1} and 4000 cm^{-1}. Over-fills in the detector due to the divergence of beam may end up with cumulative transmittance percentage of 100 ± 15% (Anvar & Mazza, 2010; Saravanakumar et al., 2013). The chopped fiber samples were grounded to fine powder using a mortar and pestle and then mixed with KBr powder. They were then pelletized by applying pressure to prepare the specimen to record the FTIR spectra. The presence of free functional groups in CQSF are determined by FTIR.

Table 1
Properties of CQRF in comparison with cellulose based natural fibers and Man-made synthetic fibers.

Fiber	Chemical properties					Physical properties					
	Cellulose (%)	Hemi cellulose (%)	Lignin (%)	Wax (%)	Moisture (%)	Density (g/cm^3)	Diameter (μm)	Gauge length (mm)	Elongation (%)	Tensile strength (MPa)	Young's modulus (GPa)
CQ stem	82.73	7.96	11.27	0.18	6.6	1.22	770–870	10–50	3.75–11.14	2300–5479	56–234
CQ root	77.17	11.02	10.45	0.14	7.3	1.51	610–725	10–50	3.57–8.37	1857–5330	68–203
Cotton	82.7	5.7	–	–	1.0	1.6	–	–	7–8	400	5–12
Coir	32–43	0.15–0.25	40–45	–	–	1.2	100–450	100	30	593	4–6
Jute	64.4	12	11.8	0.7	1.1	1.3	40–350	60	1.5–1.8	393–773	26
Flax	64.1	16.7	2.0	3.3	3.9	1.5	–	–	2.7–3.2	500–1500	27
Hemp	68	15	10	0.8	6.2	1.47	–	–	2–4	690	70
Kenaf	45–57	8–13	21.5	0.8	6–12	1.31	65–71	10	1.6	427–519	23.1–27.1
Ramie	68.6–85	13–16.7	0.5–0.7	0.3	7.5–17	1.5	50	–	2–3	220–938	44–128
Sisal	60–78	10.0–14.2	8.0–14	2.0	10–22	1.5	50–300	50	2–2.5	511–635	9–22
Pineapple leaf	70–83	–	5–12.7	–	11.8	1.4	20–80	10	0.8–1	413–1627	34–82
Banana	56–63	20–25	7–9	3	–	1.35	50–250	150	1–3.5	529–759	17.85
Palmyrah	40–52	42–43	–	–	–	1.09	70–1300	40	7–15	180–215	7–60
Bamboo	73.83	12.49	10.15	3.16	–	0.91	240–330	100	1.4	503	35.91
Sansevieria cylindrica	79.7	10.13	3.8	0.09	6.08	0.915	230–280	10–40	12.3–13.7	666–706	6–8
Sansevieria ehrenbergii	80	11.25	7.8	–	10.55	0.887	10–250	50	2.81	278.82	2.81
Curaua	70.7	9.9	7.5–11.1	–	–	1.4	170	10	3.7–4.3	500–1150	11
Bagasse	55.2	16.8	25.3	–	–	1.2	200–400	–	1.1	20–290	19–27
Phormium tenax	45.1–72	30.1	11.2	0.7	10	–	100–200	–	–	–	–
Agave	68.42	4.85	4.85	0.26	7.69	1.2	126–344	–	–	–	–
Sea grass	57	38	5	–	–	1.5	5	–	13–26.6	453–692	3.1–3.7
Alfa	45.4	38.5	14.9	2	–	0.89	–	100	5.8	350	22
Wheat straw	51	26	16	–	–	1.45	–	–	–	–	–
Oil palm	65	10.12	17.5	4	–	1.55	–	–	25	248	3.2
Henequen	60	28	6	0.5	–	1.20	–	–	3.7–5.9	430–570	11.1–16.3
Coconut tree leaf sheath	27	14	27.7	–	4.7	1.20	140–990	50	2.84	46.4	2.3
Piassava	28.6	25.8	45	–	–	1.4	–	–	7.8–21.9	134–143	1.07–4.59
Prosopis juliflora	61.65	16.14	17.11	0.61	9.48	0.58	20	–	1.77	558	–
E-glass	–	–	–	–	–	2.5	5–20	–	0.5	2000–3500	70
Aramid (std.)	–	–	–	–	–	1.4	12	–	3.3–3.7	3000–3150	63–67
Carbon (std. PAN-based)	–	–	–	–	–	1.4	8	–	1.4–1.8	4000	230–240

2.6. XRD analysis

The powdered samples were subjected to X-ray diffraction in Rigaku X-ray diffractometer D/Max Ultima III with monochromatic Cu*K*α radiation to determine the crystallinity index (CI) and crystallite size of the CQSF. The XRD analysis was carried out in 2-θ range of 10°–80° with goniometer speed of 5° min^{-1}. The integrated intensities of the Bragg peaks in the spectrum of the CQSFs were identified and their crystallinity indices were estimated.

2.7. SEM analysis of the CQSF

The surface morphology of CQSF were examined using a scanning electron microscope (HITACHI Model S3000H). The specimens were coated with a layer of platinum to avoid electron beam charging effects during examination. The SEM studies were conducted with an electron beam accelerating potential of 3 kV.

2.8. Thermo gravimetric analysis

The thermal stability behavior of the CQSF was assessed by Thermo gravimetric analysis (TGA) using Jupiter Simultaneous thermal analyser (Model STA 449 F3, NETZSCH, and Germany). To avoid oxidation effects TGA analysis were carried out in nitrogen atmosphere at a flow rate of 20 ml/min. Ten milligram of CQSFs were crushed and kept in alumina crucible to avoid the temperature variations measured by the thermocouple. The heating rate is maintained at 10 °C/min for heating it from 28 °C to 1000 °C.

3. Results and discussion

3.1. Anatomy of CQ stem and fiber

Well-developed matured CQ stem was studied for its anatomical structure through optical microscope. The stem is four angled with thick radiating arms which render the ridged internode and furrowed configuration (Fig. 2a). The central axis is about 2 to 3 mm thick. The wings are 3 mm long and 1 mm thick and the tapering ends are 500 μm thick. The stem consists of this epidermal layer of small squarish thick walled cells with prominent cuticle (Fig. 2c). The ground tissue consists of large, circular, compact thin walled parenchyma cells. The vascular strands are located in the wings of the stem. There are five vascular strands arranged in an arc in the sub marginal part of the wing (Fig. 2b), of which one median bundle is significantly larger while the other lateral strands are smaller. All the bundles are collateral comprising an outer circular mass of

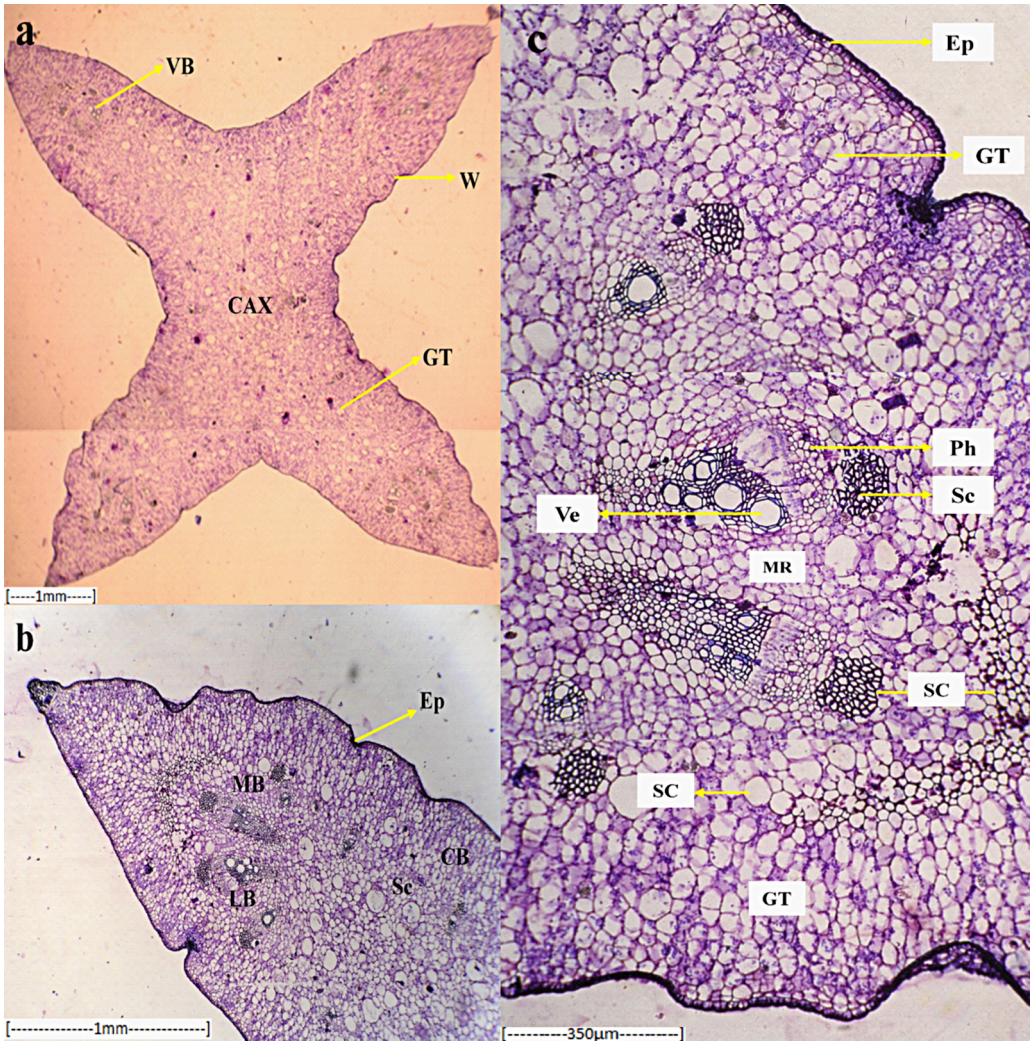

Fig. 2. Optical microscopic transverse section of *Cissusquadrangularis* stem – (a) transverse section of winged inter node entire sectional view 10×, (b) one wing enlarged 40× and (c) vascular systems of the stem—enlarged 60×. (VB—vascular bundle, W—wing, CAX—central axis, GT—ground tissue, Ep—epidermis, CB—cortical bundle, LB—lateral bundle, MB—median bundle, Sc—sclerenchyma, SC—secretory cavity, MR—medullary ray, Ph—phloem, Ve—vessels).

Table 2
Mechanical properties of *Cissus quadrangularis* stem fiber.

Gauge length (mm)	Tensile strength (MPa)	Young's modulus (GPa)	Strain to Failure %	Cross sectional area (mm^2)
10	2300 ± 735	56 ± 17	3.75 ± 2.49	0.4752 ± 0.1689
20	2823 ± 831	59 ± 19	5.46 ± 2.88	0.4661 ± 0.1598
30	3466 ± 1143	83 ± 32	7.75 ± 2.39	0.4657 ± 0.1196
40	4203 ± 1276	131 ± 37	4.78 ± 1.24	0.4229 ± 0.1262
50	4157 ± 1224	130 ± 44	6.46 ± 2.88	0.4462 ± 0.1681

sclerenchyma cap; middle mass of phloem and inner conical segment of xylem (Fig. 2c). The phloem element is wide and compact which includes sieve element and parenchymatous cells. Xylem strands consist of wide circular and angular thin walled vessels and xylem sclerenchyma (Fig. 2c). Calcium oxalate crystals of raphides are frequently seen in the ground parenchyma cells. The raphides is a thick cylindrical bundle comprising several thin pointed needles and are located alongside the elongated wide parenchyma cells. There is a wide thin arc of less prominent sclerenchyma cells overarching the five vascular strands scattered throughout the ground tissues. However, sclerenchyma cells are thick at the extreme tips of the wings (Fig. 2b). The average diameter and strength of fiber varies with aging and the plantation environment.

3.2. Chemical properties

Chemical analysis of CQSF showed high cellulose content of 82.73% which ensures good mechanical properties (Baley, 2002). The hemicellulose content is quite low (7.96%) when compared with other natural fibers. Higher levels of hemicellulose lead to disintegration of cellulose microfibrils (Morvan, Jauneau, Flaman, Millet, & Demarty, 1990) which decrease the fiber strength. Lignin constitutes 11.27% which is moderate, and it is well known for its negative influence on fiber structure and its morphology. The wax content is low at 0.18% which is good, as higher levels can lead to smooth fiber surface morphology and reduce the bonding capacity of the fiber with the matrix.

3.3. Physical properties

3.3.1. Fiber density

The investigated CQSF was found to have an average density of 1.22 g/cm^3 which is significantly lower than widely used synthetic fibers such as E-glass fiber (2.56 g/cm^3) and carbon fiber (1.4–1.8 g/cm^3) (Rita, Sarkar, & Bose, 2001). The specific strength of CQSF is very high with an average value of 3445 kNm/kg in comparison with synthetic fibers.

3.3.2. Tensile behavior of the CQSF

The average fiber diameter was determined from 30 samples through optical microscope images taken in the longitudinal direction using Image-pro software (Indran et al., 2014). Table 2 shows that the tensile strength and Young's modulus values, which increases with increase in gauge lengths from 10 mm to 40 mm. As the gauge length increases the deviation from the mean value for various samples increases, which was expected for any natural fiber characterization. The variation in Young's modulus was rather high which is due to artifacts.

3.4. FTIR analysis

FTIR spectra show eight well-defined peaks of CQSFs at 3328, 2922, 2342, 1663, 1609, 1313, 1030 and 778 cm^{-1} (Fig. 3a). The peak at 3328 cm^{-1} belongs to the carboxylic acid O—H stretching due to the presence of cellulose I (Jayaramudu, Guduri, & Varada Rajulu, 2010) and sp^3 C—H stretching occurred due to the vibration of cellulose, which is noted by a moderate peak at 2922 cm^{-1} (Kiruthika & Veluraja, 2009). The peak at 2342 cm^{-1} in the CQSF indicates the presence of C≡C alkynes group. A small peek at 1663 cm^{-1} is attributed to the presence of alkene carboxyl group of C=C stretching, which shows the presence of hemicellulose. The smaller peak indicates less percentage content of hemicellulose, which is advantageous, because higher content will affect the mechanical properties of CQSFs. The peak at band 1609 cm^{-1} indicates the C=C aromatic stretching with strong conjugated C—C bond and this peak is attributed to lignin content in the fiber (Saravanakumar et al., 2013). Similarly, the peak at 1313 cm^{-1} band is ascribed to strong acyl C—O with overlapped C—H stretching of phenols and esters. The band 1030 cm^{-1} corresponds to alkoxy C—O ordinary bond bending vibration (Venkata Prasad et al., 2010; Saravanakumar et al., 2013) and the smaller peak at 778 cm^{-1} represent the presence

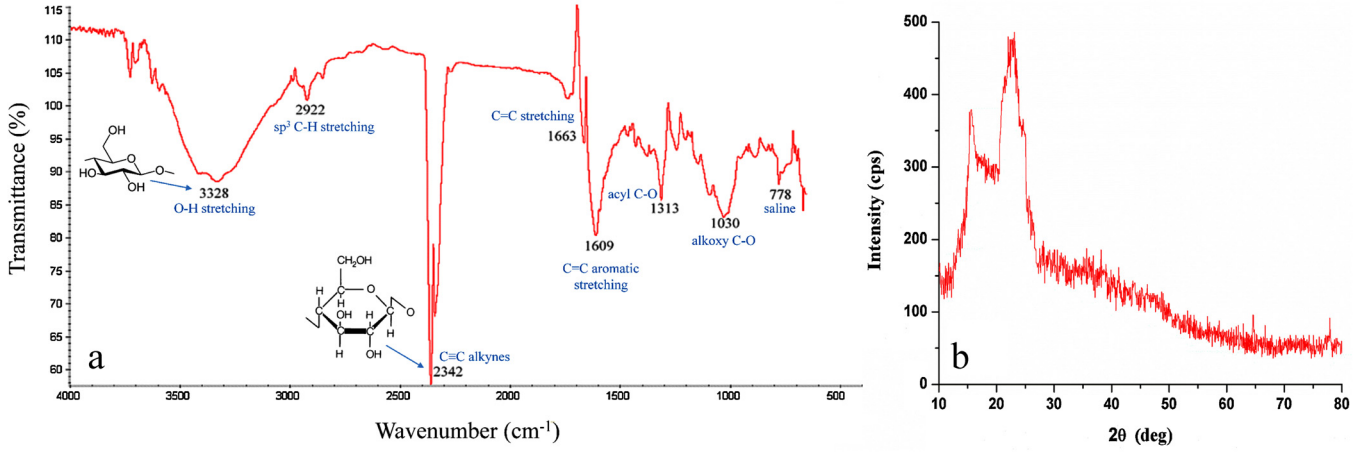

Fig. 3. (a) FTIR and (b) XRD spectrum of the CQSF.

of saline content (Khan & Drzal, 2004). The natural fiber bands can vary around $\pm 16\,cm^{-1}$ from their position for different studies (Zhbankov et al., 2002).

3.5. XRD analysis

The XRD spectrum of the investigated CQSF showed two major peaks at 15.7° and 22.85° which are ascribed to the presence of cellulose type I, exhibiting monoclinic structure (Fig. 3b). These peaks can be further related to the crystallographic planes (2 0 0) and $(1\bar{1}0)$, respectively (Sreenivasan et al., 2011). The CI was calculated using the expression (2) as 47.15%, where $H_{22.85}$ and $H_{18.5}$ are the height of the peaks at 22.85° and 18.5°, respectively.

$$CI = \frac{H_{22.85} - H_{18.5}}{H_{22.85}} \quad (2)$$

$H_{18.5}$ is the diffraction intensity 18.5° which is related to the amorphous fraction and $H_{22.85}$ is that of the crystalline fraction. The CI of various natural fibers reported are *Wrighitia tinctoria* seed fiber (49.2%), ramie fiber (58%), *Sansevieria cylindrica* leaf fibers (60%), *Raffia textilis* (64%), sisal (71%), jute (71%), flax (80%) and hemp (88%) (Sreenivasan et al., 2011). The crystallite size (L) was estimated using Scherrer's formula (Elenga, Dirras, Goma Maniongui, Djemia, & Biget, 2009; D'Almeida, Aquino, & Monteiro, 2006):

$$L = \frac{K\lambda}{\beta \cos\theta} \quad (3)$$

where $K = 0.89$ is Scherrer's constant, β is the peak's full-width half-maximum (FWHM) and λ is the wavelength of the radiation. The crystalline size was calculated as 31.55 nm for the first crystallographic plane (2 0 0) and that of the second crystallographic plane $(1\bar{1}0)$ is 3.91 nm. The crystallite size for some natural fibers are *R. textilis* (32 nm), ramie fibers (16 nm), cotton fibers (5.5 nm), corn stalk fibers (3.8 nm) and flax fibers (2.8 nm) (Sreenivasan et al., 2011; Reddy & Yang, 2005).

3.6. Surface morphology

The surface morphology of a fiber is a very important factor in determining the ability of the fiber to act as a good reinforcement and to resist fiber pull out. Images from the scanning electron microscope (SEM) reveal the presence of shallow pores which increases the surface roughness of the fiber (Fig. 4). The surface roughness contributes for increased contact surface area to ensure better adherence of the fiber with the matrix in composite manufacturing. The presence of starch grains and impurities are noted, which can be cleaned by pre-casting fiber treatments. The presence of complex structured lateral pores provides the extra stiffness to this fiber. The microfibril angle (α) was also calculated using the global deformation equation (4) as 4.95° ± 0.32.

$$\varepsilon = \ln\left[1 + \frac{\Delta L}{L_o}\right] = -\ln(\cos\alpha) \quad (4)$$

where ε is the strain, α is the microfibril angle in degree, $\left[\Delta L/L_o\right]$ is the ratio of elongation. The reported microfibril angle for jute, flax, hemp, banana and *Prosopis juliflora* fibers are 8.1°, 5°, 6.2°, 11–12° and 10.64°, respectively (Kulkarni, Satyanarayana, & Rohatgi, 1983; Perry, 1975; Saravanakumar et al., 2013). Lower microfibril angle gives better mechanical properties.

3.7. Thermal analysis

Fig. 5a shows the TGA and DTG curves of the investigated CQSF. The first drop in mass was noted at 89 °C which is attributed to the removal of moisture and wax. The next drop occurring at 294 °C, indicate the degradation of hemicellulose and glycosidic links of

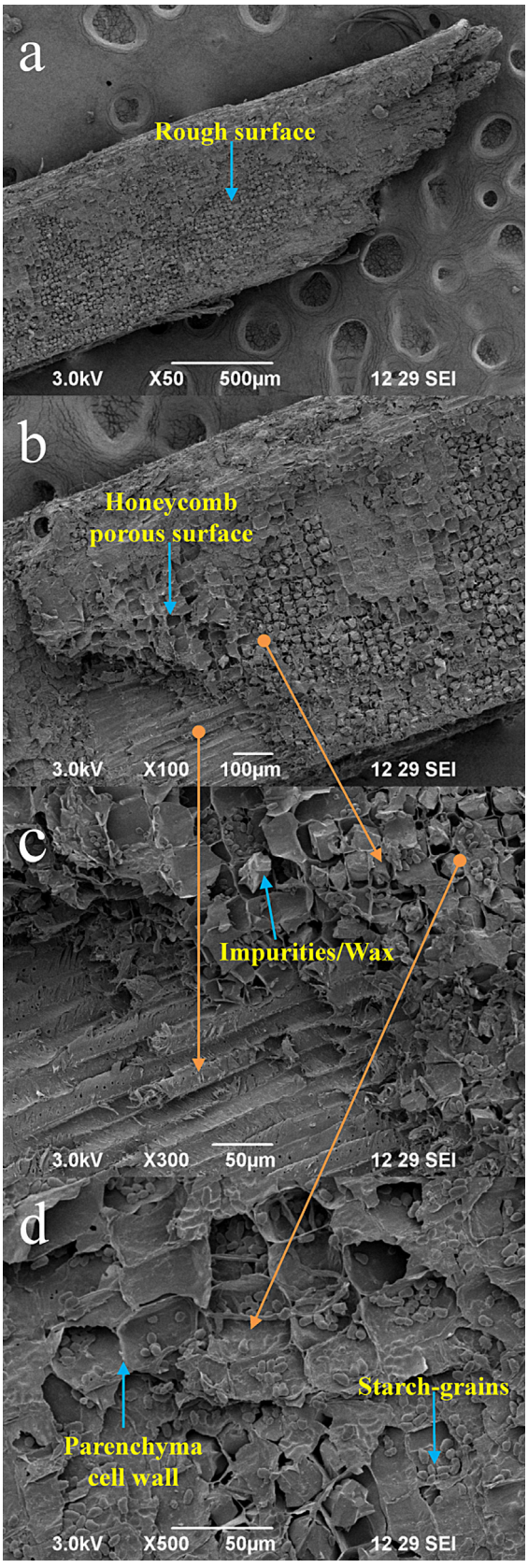

Fig. 4. Scanning electron micrographs of *Cissusquadrangularis* stem–(a) 50×, (b) 100×, (c) 300× and (d) 500×.

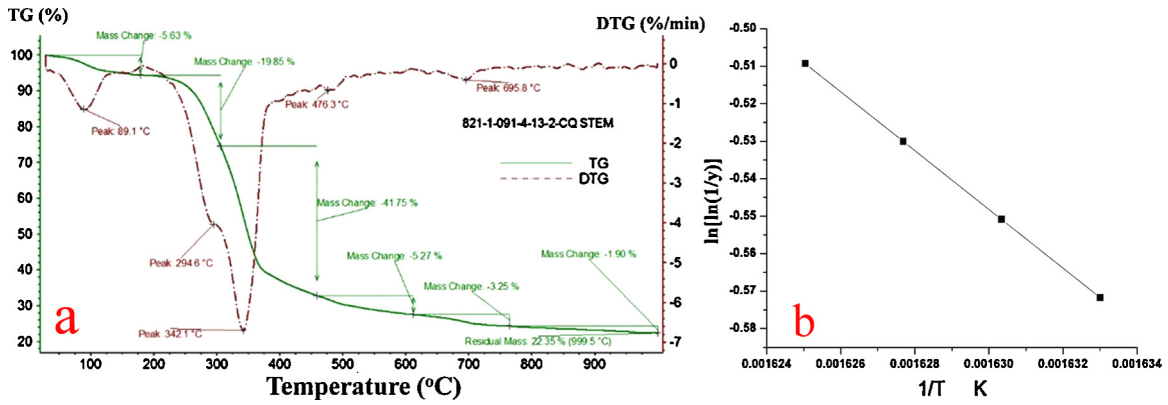

Fig. 5. Thermal analysis (a) TG and DTG curves of the CQSF, (b) Broido's plot of the CQSF.

Table 3
Degradation temperature of CQSF along with other man-made and natural fibers.

Weight loss %	T (°C) 5%	T (°C) 25%	T (°C) 50%	T (°C) 75%
CQSF	91	345	405	495
CQRF	88	328	395	481
Hemp	104	329	341	457
Kenaf	64.3	313	340	370
Henquen	61	301	337	391
Flax	88	322	338	441
Prosopis juliflora	110	331	380	480
Jute	60	290	340	470
Sisal	52	275	345	465
Wood	107	270	367	400
Cotton	55	280	330	410
Glass*	586			

* Ultimate fiber weight loss was 1.6%.

cellulose and the subsequent third and largest drop was noted at 342 °C where the fiber starts to burn and the α-cellulose degrades (Sgriccia & Hawley, 2007; Azwa, Yousif, Manalo, & Karunasena, 2013). Similar drops were reported for various other fibers such as bamboo, hemp, jute, and Kenaf at 321 °C, 308 °C, 298 °C, and 307 °C, respectively (Saravanakumar et al., 2013). Further, the less prominent drops at 476 °C and 695 °C are the result of lignin degradation and oxidative degradation of charred residue of the fiber. At the end of the process, 22.35% of the mass was found remaining at a temperature of 999 °C. Degradation temperature of man-made E-glass fiber and some natural fibers were also listed in Table 3 (Sgriccia & Hawley, 2007; Saravanakumar et al., 2013; Indran et al., 2014). The apparent activation energy, E_a was calculated to know the kinetic parameter of CQSF (Das and Chakrabarty, 2008) using the Broido's equation:

$$\varepsilon = \ln\left[\ln\left[\frac{1}{y}\right]\right] = -\left(\frac{E}{R}\right)\left[\left(\frac{1}{T}\right) + K\right] \quad (5)$$

where R is the universal gas constant (8.314 J/mol K), T is the temperature in Kelvin, y is the normalized weight (w_t/w_o), w_t symbolizes the weight of the sample at any time t, whereas w_o indicates the initial sample weight. The kinetic activation energy E_a = 65.23 kJ/mol was interpolated from the Broidio's plot of ln[ln (1/y)] verses (1/T) in Kelvin (Fig. 5b). The activation energy of CQSF is within the range specified for natural materials, i.e., 60–170 kJ/mol, which signifies that the CQSF fiber has thermal stability to withstand polymerization process temperature in making fiber reinforced polymer composite (Saravanakumar et al., 2013).

4. Conclusion

The characterization of CQSF provides new hope for natural fiber research to compete with hazardous synthetic fiber with its excellent properties. The density of CQSF is significantly lower than that of the popular glass fiber, carbon fiber, etc. and also gives 20% better specific strength. The tensile strength and Young's modulus are 4203 ± 1276 MPa and 131 ± 37 GPa which is significantly higher than any other natural fibers ever investigated and also on par with widely used synthetic fibers. The high cellulose content (82.73%) and lower lignin content (11.27%) ensure better mechanical strength. The honey comb surface morphology and lower wax content (0.18%) enhance the bonding strength when they are used as reinforcement for composite manufacturing. The thermal analysis confirms its stability to withstand polymerization temperature. Thus this characterization results firmly confirms the possibility of using this fiber for the manufacture of sustainable fiber reinforced polymer composite.

Acknowledgement

The first author acknowledges the Department of Science and Technology, Government of India for providing INSPIRE fellowship to carry out his research work.

References

Anvar, U. B., & Mazza, G. (2010). Extraction and characterization of hemicelluloses from flax shives by different methods. *Carbohydrate Polymers*, *79*, 17–25.
Azwa, Z. N., Yousif, B. F., Manalo, A. C., & Karunasena, W. (2013). A review on the degradability of polymeric composites based on natural fibres. *Materials and Design*, *47*, 424–442.
Baley, C. (2002). Analysis of the flax fibers tensile behavior and analysis of the tensile stiffness increase. *Composites, A: Applied Science and Manufacturing*, *33*, 939–948.
Béakou, A., Ntenga, R., Lepetit, J., Atéba, J. A., & Ayina, L. O. (2008). Physico-chemical and microstructural characterization of "Rhectophyllum camerunense" plant fiber. *Composites, A: Applied Science and Manufacturing*, *39*, 67–74.
Cavallo, D., Campopiano, A., Cardinali, G., Casciardi, S., Simone, D. P., Kovacs, D., et al. (2004). Cytotoxic and oxidative effects induced by man-made vitreous fibers (MMVFs) in a human mesothelial cell line. *Toxicology*, *201*, 219–229.
Conrad, C. M. (1944). Determination of wax in cotton fiber: A new alcohol extraction method. Industrial and engineering chemistry. *Analytical Edition*, *16*, 745–748.
Das, M., & Chakrabarty, D. (2008). Thermo gravimetric analysis and weathering study by water immersion of alkali-treated bamboo strips. *Bio Resource*, *3*, 1051–1062.
D'Almeida, J. R. M., Aquino, R. C. M. P., & Monteiro, S. N. (2006). Tensile mechanical properties, morphological aspects and chemical characterization of piassava (Attala funifera) fibers. *Composites, A: Applied Science and Manufacturing*, *37*, 1473–14739.
Dittenber, D. B., & Ganga Rao, H. V. S. (2012). Critical reviews of recent publications on use of natural composites in infrastructure. *Composites, A: Applied Science and Manufacturing*, *43*, 1419–1429.
Doree, C. (1950). *The methods of cellulose chemistry* (2nd ed.). London: Chapman and Hall.
Elenga, R. G., Dirras, G. F., Goma Maniongui, J., Djemia, P., & Biget, M. P. (2009). On the microstructure and physical properties of untreated *Raffia textilis* fiber. *Composites, A: Applied Science and Manufacturing*, *40*, 418–422.
Faruk, O., Bledzkia, A. K., Finkb, H., & Sain, M. (2012). Biocomposites reinforced with natural fibers 2000–2010. *Progress in Polymer Science*, *37*, 1552–1596.

Pacheco-Torgal, Fernando, & Jalali, S. (2011). Cementitious building materials reinforced with vegetable fibres: A review. *Construction and Building Materials*, *25*, 575–581.
Hejazi, S. M., Sheikhzadeh, M., Abtahi, S. M., & Zadhoush, A. (2012). A simple review of soil reinforcement by using natural and synthetic fibers. *Construction and Building Materials*, *30*, 100–116.
Ho, M., Wang, H., Lee, J., Ho, C., Lau, K., Leng, J., et al. (2012). Critical factors on manufacturing processes of natural fibre composites. *Composites, B: Engineering*, *43*, 3549–3562.
Indran, S., Raj, R. E., & Sreenivasan, V. S. (2014). Characterization of new natural cellulosic fiber from *Cissus quadrangularis* root. *Carbohydrate Polymers*, *110*, 423–429.
Jawaid, M., & Abdul Khalil, H. P. S. (2011). Cellulosic/synthetic fibre reinforced polymer hybrid composites: A review. *Carbohydrate Polymers*, *86*, 1–18.
Jayant, H. M., & Palit, P. (2013). Biology of industrial bast fibers with reference to quality. *Journal of Natural Fibers*, *10*, 176–196.
Jayaramudu, J., Guduri, B. R., & Varada Rajulu, A. (2010). Characterization of new natural cellulosic fabric Grewia tilifolia. *Carbohydrate Polymers*, *79*, 847–851.
Khan, M. A., & Drzal, L. T. (2004). Characterization of 2-hydroxyethyl methacrylate (HEMA)—Treated jute surface cured by UV radiation. *Journal of Adhesion Science and Technology*, *18*, 381–393.
Kiruthika, A. V., & Veluraja, K. (2009). Experimental studies on the physico-chemical properties of banana fibre from various varieties. *Fibers and Polymers*, *10*, 193–199.
Koronis, G., Silva, A., & Fontul, M. (2013). Green composites: A review of adequate materials for automotive applications. *Composites, B: Engineering*, *44*, 120–127.
Ku, H., Wang, H., Pattarachaiyakoop, N., & Trada, M. (2011). A review on the tensile properties of natural fiber reinforced polymer composites. *Composites, B: Engineering*, *42*, 856–873.
Kulkarni, A. G., Satyanarayana, K. G., & Rohatgi, P. K. (1983). Mechanical properties of banana fibers (Musa Sepientum). *Journal of Materials Science*, *18*, 2290–2296.
Mantia, F. P. L., & Morreale, M. (2011). Green composites: A brief review. *Composites, A: Applied Science and Manufacturing*, *42*, 579–588.
Mehta, G., Mohanty, A. K., Misra, M., & Drzal, I. T. (2004). Effect of novel sizing on the mechanical and morphological characteristics of natural fiber reinforced unsaturated polyester resin based bio-composites. *Journal of Materials Science*, *39*, 2961–2964.
Morvan, C., Jauneau, A., Flaman, A., Millet, J., & Demarty, M. (1990). Degradation of flax polysaccharides with purified endo-polygalacturonase. *Carbohydrate Polymers*, *13*, 149–163.
O'Brien, T. P., Feder, N., & McCull, M. E. (1964). Polychromatic staining of plant cell walls by toludine blue—O. *Protoplasma*, *59*, 364–373.
Pearl, I. A. (1967). *The chemistry of lignin*. New York, NY: Marcel Dekker (Chapter 4).
Perry, D. R. (1975). *Identification of textile materials* (7th ed.). London: The Textile Institute, Manara Printing Services.
Reddy, K. O., Uma, M. C., Mukul, S., Song, J. I., & Varada Rajulu, A. (2013). Tensile and structural characterization of alkali treated *Borassus* fruit fine fibers. *Composite, B: Engineering*, *44*, 433–438.
Reddy, N., & Yang, Y. (2005). Structure and properties of high quality natural cellulose fibers from cornstalks. *Polymer*, *46*, 5494–5500.
Rita, R., Sarkar, B. K., & Bose, N. R. (2001). Behaviour of E-glass fibre reinforced vinyl ester resin composites under impact fatigue. *Bulletin of Material Science*, *24*, 137–142.
Saravanakumar, S. S., Kumaravel, A., Nagarajan, T., Sudhakar, P., & Baskaran, R. (2013). Characterization of a novel natural cellulosic fiber from *Prosopis juliflora* bark. *Carbohydrate Polymers*, *92*, 1928–1933.
Sass, J. E. (1940). *Elements of botanical micro technique* (1st ed.). New York, NY: McGraw Hill Book Co.
Sathishkumar, T. P., Navaneethakrishnan, P., Shankar, S., Rajasekar, R., & Rajini, N. (2013). Characterization of natural fiber and composites—A review. *Journal of Reinforced Plastics and Composites*, *32*, 1457–1476.
Sathishkumar, T. P., Navaneetha krishnan, P., & Shankar, S. (2012). Tensile and flexural properties of snake grass natural fiber reinforced isophthallic polyester composites. *Composites Science and Technology*, *72*, 1183–1190.
Satyanarayana, K. G., Sukumaran, K., Mukherjee, R. S., Pavithran, C., & Pillai, S. G. K. (1990). Natural fibre-polymer composites. *Cement and Concrete Composites*, *12*, 117–136.
Satyanarayana, K. G., Flores-Sahagunb, Thais H. S., Lucas, P. D. S., & Juliana, D. S. (2013). Characterization of blue agave bagasse fibers of Mexico. *Composites, A: Applied Science and Manufacturing*, *45*, 153–161.
Sgriccia, N., & Hawley, M. C. (2007). Thermal, morphological, and electrical characterization of microwave processed natural fiber composites. *Composites Science and Technology*, *67*, 1986–1991.
Sreenivasan, V. S., Somasundaram, S., Ravindran, D., Manikandan, V., & Narayanasamy, R. (2011). Microstructural, physico-chemical and mechanical characterization of *Sansevieria cylindrica* fibres—An exploratory investigation. *Materials and Design*, *32*, 453–461.
Thiruchitrambalam, M., Athijayamani, A., Sathiyamurthy, S., & Syed Abu Thaheer, A. (2010). A review on the natural fiber-reinforced polymer composites for the development of roselle fiber-reinforced polyester composite. *Journal of Natural Fibers*, *7*, 307–323.
Tulinska, J., Eva, J., Maria, D., Miroslava, K., et al. (2004). Immunomodulatory effects of mineral fibers in occupationally exposed workers. *Mutation Research*, *553*, 111–124.
Venkata Prasad, C., Chowdoji Rao, K., Venkata Reddy, G., Sobha Rani, T., Yerriswamy, B., & Subha, M. C. S. (2010). Characteristic studies of ligno-cellulosic fabric Grewia tenax. *Journal of Natural Fibers*, *7*, 194–215.
Zhbankov, R. G., Firsov, S. P., Buslov, D. K., Nikonenko, N. A., Marchewka, M. K., & Ratajczak, H. (2002). Structural physico-chemistry of cellulose macro molecules. Vibrational spectra and structures of cellulose. *Journal of Molecular Structure*, *614*, 117–125.